ELECTROPHYSIOLOGY OF A DENDRITIC NEURON MODEL

WILFRID RALL

From the Office of Mathematical Research, National Institute of Arthritis and Metabolic Diseases, National Institutes of Health, Bethesda

INTRODUCTION

The development of a mathematical model of dendritic neurons was begun because of a need to combine three different kinds of knowledge into a coherent theory. First, we have the anatomical concept of the neuron, together with the anatomical fact that extensive dendritic branching is characteristic of many important neuron types. Second, we have the theoretical development of the nerve membrane models that Dr. Cole[1] has just reviewed for you. Finally, we have a detailed body of quantitative electrophysiological information that has been obtained from individual neurons by means of intracellular and extracellular microelectrodes. I doubt that any biophysicist will be surprised to be told that a mathematical model is essential to the development of a neuron theory that aims to satisfy simultaneously these three kinds of information.

There are further objectives of such a neuron model that also deserve to be mentioned. The integration of synaptic excitation and inhibition at the neuronal level can be subjected to theoretical analysis in terms of such a model. This, in turn, has relevance to the next level of theoretical neurophysiology, namely, inter-actions between several neurons and also between large populations of neurons. The dendritic neuron model may even have relevance to the problem of learning.

Having made that speculative remark, I now return to the well-established anatomical facts of dendritic branching. Three important examples of such branching are illustrated in Fig. 1. These illustrations have been reproduced from the work of Ramón y Cajal (1909), of more than fifty years ago; their validity has been confirmed by many histologists. I show them today to remind you that branching can be very extensive. In the case of the Purkinje cell, detailed measurements (Fox and Barnard, 1957) yield an estimate that the dendritic surface area is as much as eighty to one hundred times that of the soma; in the case of motoneurons or pyramidal cells of cat, the dendritic surface area has been estimated to be as much as ten

[1] See preceding paper by Dr. K. S. Cole.

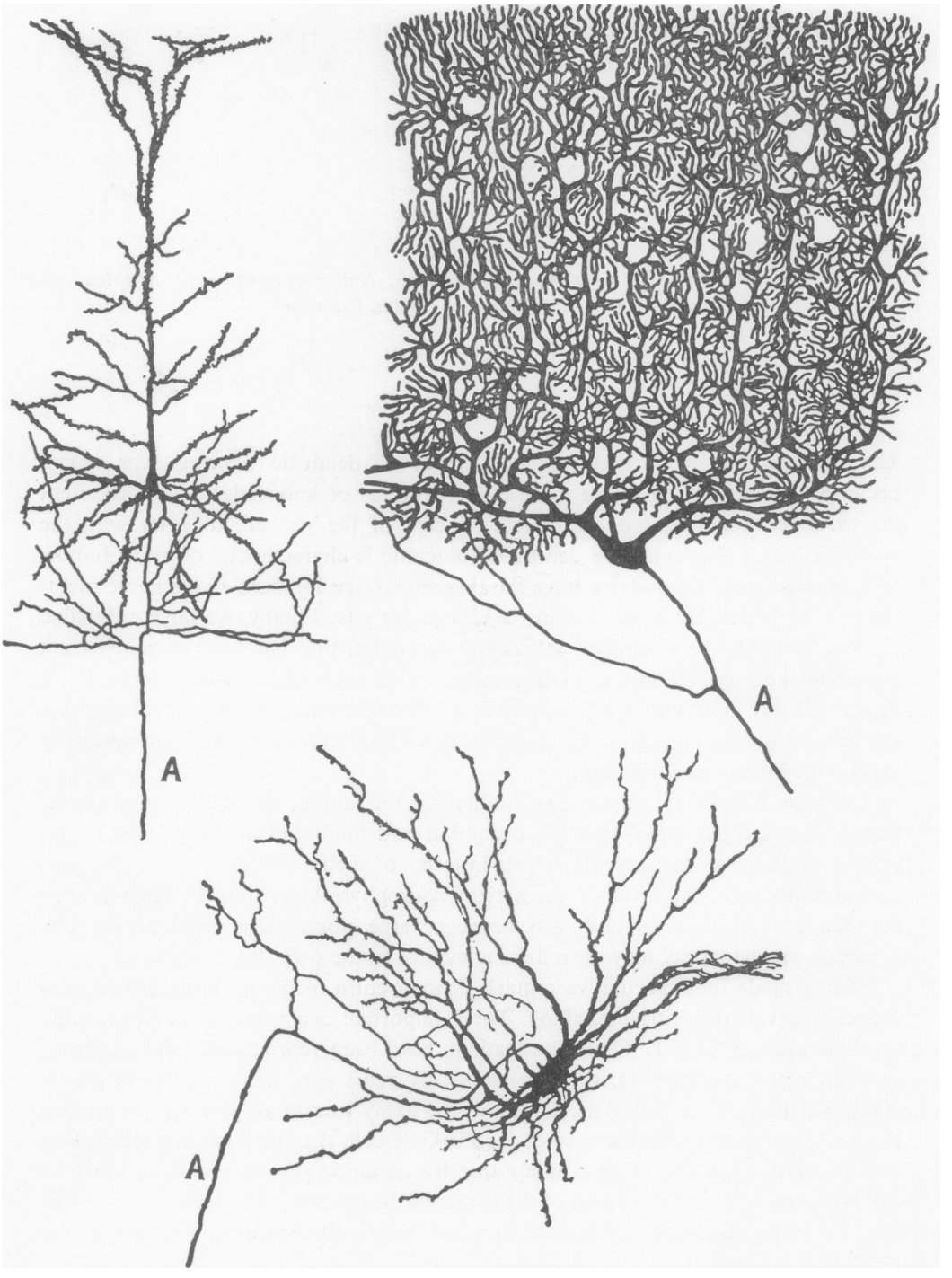

FIGURE 1 Pyramidal cell of cerebral cortex shown upper left. Purkinje cell of cerebellum shown upper right. Motoneuron of spinal cord shown below. In each case, the letter, *A*, indicates the axon, which is cut off. These illustrations are reproduced with only slight modification from the classic work of Ramón y Cajal (1909).

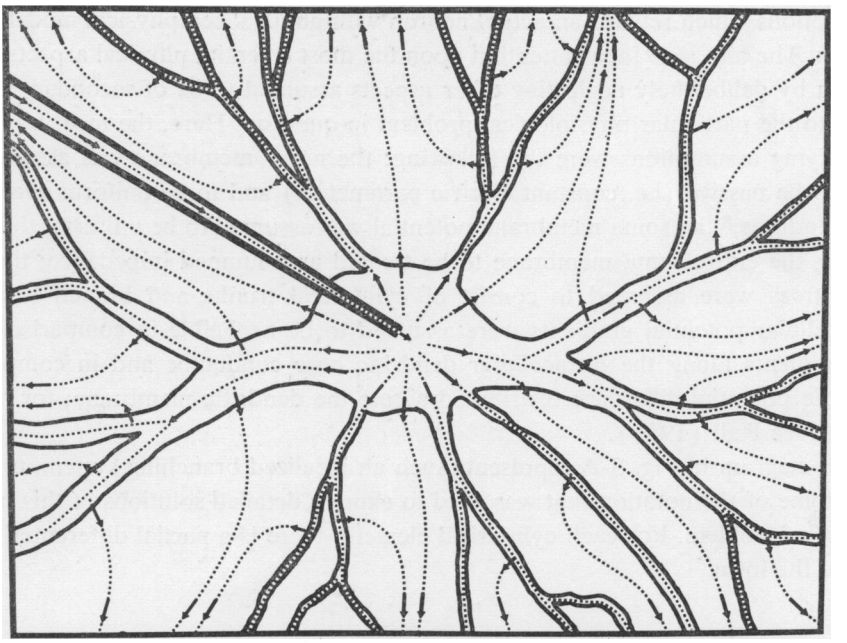

FIGURE 2 Diagram illustrating the flow of electric current from a microelectrode whose tip penetrates the cell body (soma) of a neuron. The full extent of the dendrites is not shown. The external electrode to which the current flows is at a distance far beyond the limits of this diagram.

or twenty times that of the soma (Sholl, 1955 b; Aitken, 1955; Young, 1958; cf., Aitken and Bridger, 1961). Neurophysiologists have recently begun to place increasing emphasis on the importance of this extensive dendritic surface to the receptive and integrative functions of the neuron (see Bishop, 1958; Bullock, 1959; Rall, 1961).

The next figure (Fig. 2) provides a diagrammatic illustration of the kind of problem that was introduced by the use of intracellular microelectrodes for stimulation and recording in dendritic neurons. When electric current flows from such an intracellular electrode to a distant external electrode, it can be estimated that only a small portion of the total steady current flows directly across the soma membrane, and that a much larger portion of current flows into the several dendritic trees and then out across the extensive dendritic membrane surface. Thus, it can be seen that the skillful techniques employed by the experimental neurophysiologists (e.g., Coombs, Eccles and Fatt, 1955; Araki and Otani, 1955; Frank and Fuortes, 1956), created a theoretical challenge for satisfactory methods of interpretation.

THE MODEL

The first step in treating this problem theoretically is to make several simplifying

assumptions which replace an actual neuron with an idealized physical model of the neuron. The aim is to focus attention upon the most essential physical aspects of the neuron by deliberately neglecting other aspects assumed to be of secondary importance to the particular physiological problem in question. Here, the most important simplifying assumptions were the following: the nerve membrane was assumed, at first, to be passive (i.e. constant electric parameters) and to be uniform over soma and dendrites;[2] the soma membrane potential was assumed to be uniform, thus permitting the entire soma membrane to be treated as a lumped impedance; the dendritic trees were assumed to consist of cylindrical trunks and branch elements; extracellular potential gradients were assumed to be negligible in comparison with the gradients along the intracellular dendritic core conductor and in comparison with the potential difference distributed across the dendritic membrane; for further details, see Rall (1959).

The diagram in Fig. 3-A represents such an idealized branching system, together with some of the notation that was used to express detailed solutions of this boundary value problem. For each cylindrical element, there is a partial differential equation of the form

$$\frac{\partial^2 V}{\partial X^2} = V + \frac{\partial V}{\partial T}$$

where V represents the deviation of the membrane potential from its resting value, $T = t/\tau$ expresses the time in terms of the passive membrane time constant, and $X = x/\lambda$ expresses distance along the cylinder in terms of its characteristic length. This equation is well-established for axons (e.g., Hodgkin and Rushton, 1946; Davis and Lorente de Nó, 1947); here we require solutions appropriate to cylinders of finite length, with boundary conditions determined by the physical requirement of continuity for both membrane potential and core current at all points of junction. A systematic method of satisfying all of these boundary conditions for any arbitrary branching pattern under steady state conditions has been presented in detail (Rall, 1959).

In order to treat transient solutions in dendritic trees, it is very useful to consider the class of dendritic trees which is electrotonically equivalent to a cylinder, and to consider also a larger class that is considerably more general than this. For this purpose, we make use of a mathematical transformation which amounts to a replacement of the usual electrotonic distance, $X = x/\lambda$, by what might be called a generalized electrotonic distance,

$$Z = \int_0^x \frac{ds}{\lambda},$$

[2] Specific relaxations of this assumption are made for certain purposes. For example, explicit conductances are added in Fig. 5 in order to approximate synaptic excitation and inhibition; in Fig. 6 these conductances have been assumed to be non-uniform in the sense of two regions. Also, in Figs. 7, 9 and 10, the soma membrane is assumed to generate an action potential.

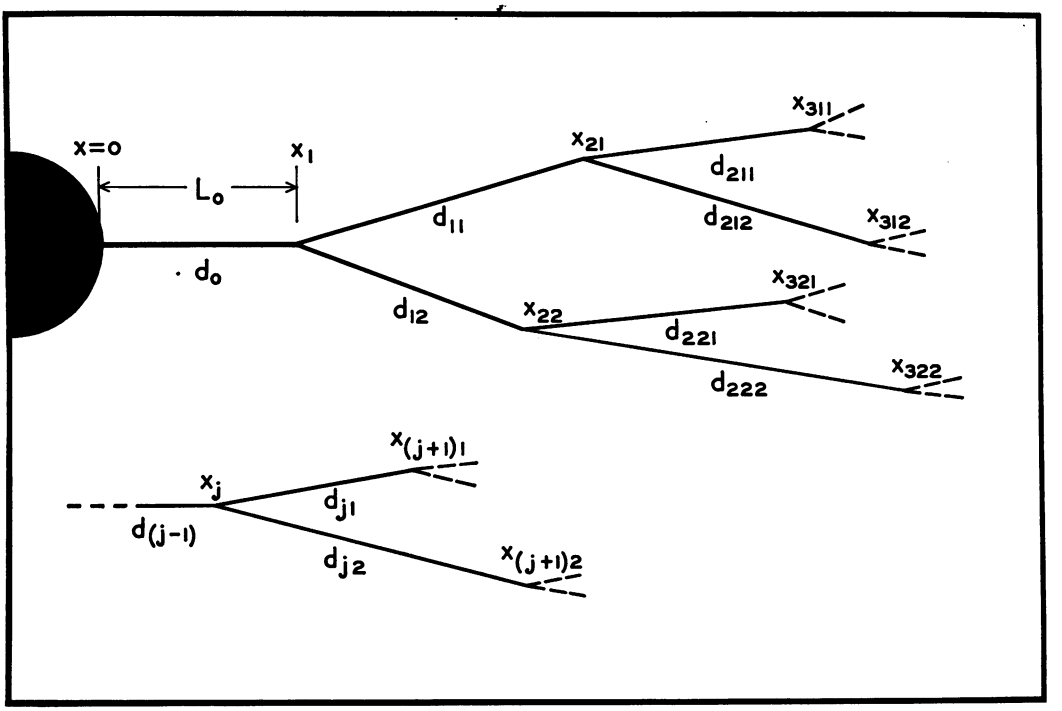

FIGURE 3-A Dendritic branching diagrams to illustrate the subscript notation used in the treatment of arbitrary branching patterns (see, Rall, 1959).

where λ depends upon branch diameter, and x represents distance (measured along the successive axes of dendritic trunk and branches) from the point of trunk origin at the soma.[3] In terms of this generalized electrotonic distance, the partial differential equation describing passive membrane electrotonus in a branching dendritic tree is found to simplify to the form

$$\frac{\partial^2 V}{\partial Z^2} + K\frac{\partial V}{\partial Z} = V + \frac{\partial V}{\partial T}$$

provided that the dendritic branching satisfies the relation

$$\sum_j (d_j)^{3/2} = (d_0)^{3/2} e^{KZ}$$

where K is a constant, d_j represents the diameter of the j^{th} branch at any given value of Z, and the summation over j exhausts all branches at each particular value of Z. For the special case, $K = 0$, the partial differential equation reduces to the same form

[3] Here cylindrical branches are assumed, and the value of λ is expected to decrease (as a step function of x) in proportion to the square root of branch diameter. A more general definition that provides also for continuous taper of branch diameter has been used in a more detailed presentation of this problem (Rall, 1961, equations 18 and 27).

as for the cylinder, except that the electrotonic distance, X, has been replaced by the generalized electrotonic distance, Z. Thus, any dendritic tree corresponding to $K = 0$ can be regarded as electrotonically equivalent to an unbranched cylinder whose length is expressed in units of Z; this fact is illustrated diagrammatically in Fig. 3-B, which is based upon the specific numerical example tabulated elsewhere (Rall, 1961, Table I). It is an important property of such dendritic trees that equal increments in Z correspond to equal increments in branching surface area, as well as equal increments of electrotonic distance.

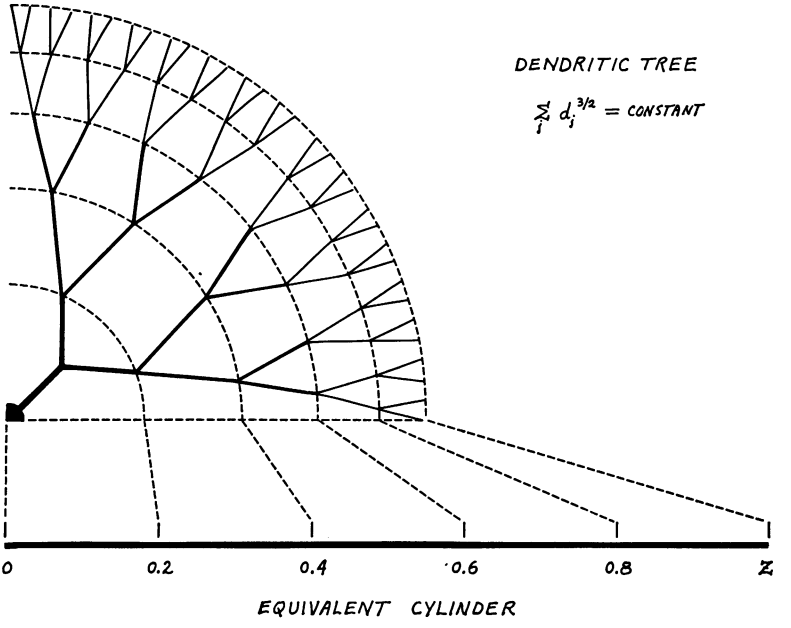

FIGURE 3-B Diagram illustrating electrotonic equivalence between a cylinder and a branching dendritic tree whose branching is such that the sum of the 3/2 power of branch diameter is constant for all values of Z (i.e., the class corresponding to $K = 0$; see text). This particular dendritic tree is intended to correspond to the specific numerical example presented elsewhere (Rall, 1961, Table I, with a radial extent of 825 microns). The dotted lines indicate the correspondence of increments of the branching tree with increments of Z in the equivalent cylinder.

The more general class of dendritic trees, corresponding to positive and negative values of the constant, K, includes a very wide range of profuseness or paucity of branching.

CURRENT STEP APPLIED AT SOMA

When a current step is applied across the soma membrane, the dendritic neuron model can be used to calculate theoretical transient responses of the form illustrated

in Fig. 4. Here it is assumed that the dendritic trees are electrotonically equivalent to passive membrane cylinders of infinite length.[4] The dendritic contribution to the transient is shown by the uppermost curve in Fig. 4; this curve is defined by $V = \text{erf}\ \sqrt{t/\tau}$, as is already well established in the theory of axonal electrotonus. This transient is significantly faster than the simple exponential transient, $1 - e^{-t/\tau}$ (see lowermost curve in Fig. 4), that would be expected for a soma without any dendrites. The intermediate curves correspond to various factors of dendritic domi-

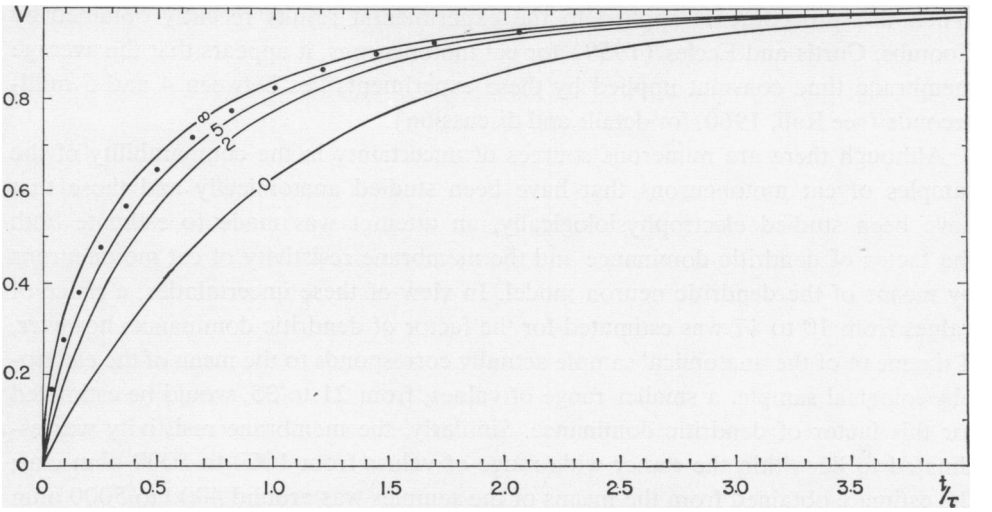

FIGURE 4 Transients of passive soma membrane potential when a constant current step is applied across the soma membrane at zero time. The electrotonic potential, V, is expressed relative to its final steady value during constant applied current. Time is expressed relative to the membrane time constant. Curves are drawn for $\rho = 0$, 2, 5 and ∞; the dots correspond to $\rho = 10$, where ρ represents the factor of dendritic dominance; see Rall (1960, equation 9). The uppermost curve, $\rho = \infty$, represents the limiting case in which the dendrites are completely dominant. The lowermost curve, $\rho = 0$, represents the limiting case of a soma without dendrites.

nance, as expressed by the steady state ratio of combined dendritic input conductance to soma membrane conductance.

Because of practical difficulties in fitting these theoretical transients to experimental results, it is useful to note that in the case of complete dendritic dominance, the

[4] The mathematical statement of this problem, and its solution by means of the Laplace transformation, are given by Rall (1960, pp. 523–526). For equivalent dendritic cylinders of finite length, a mathematically different class of transient solutions has been obtained; it consists of a convergent series of exponential terms. Preliminary numerical calculations indicate that, for finite lengths greater than about four, in units of Z, there is little numerical difference between the two classes of transient solutions. In the future, especially if anatomical and electrophysiological measurements are made on the same cell, it would be desirable to estimate the extent of the dendritic trees in terms of Z and K, and to make use of the transient solution corresponding to finite length.

slope, dV/dt, of the theoretical transient is proportional to the quantity, $(e^{-t/\tau})/\sqrt{t}$. This provides the basis for the following simple procedure for the analysis of such transients:

$$\text{plot } \log_e [\sqrt{t}\,(dV/dt)], \text{ versus } t.$$

The result should be a straight line; the negative slope of this line gives the reciprocal of the membrane time constant. It has also been shown that this simple procedure provides a good approximation even for rather small factors of dendritic dominance. When this procedure is applied to the experimental results recently obtained by Coombs, Curtis and Eccles (1959) for cat motoneurons, it appears that the average membrane time constant implied by these experiments lies between 4 and 5 milliseconds (see Rall, 1960, for details and discussion).

Although there are numerous sources of uncertainty in the comparability of the samples of cat motoneurons that have been studied anatomically and those that have been studied electrophysiologically, an attempt was made to estimate both the factor of dendritic dominance and the membrane resistivity of cat motoneurons by means of the dendritic neuron model. In view of these uncertainties, a range of values from 10 to 47 was estimated for the factor of dendritic dominance; however, if the mean of the anatomical sample actually corresponds to the mean of the electrophysiological sample, a smaller range of values, from 21 to 35, would be estimated for this factor of dendritic dominance. Similarly, the membrane resistivity was estimated to lie within the rather wide range of values from 1000 to 8000 ohm cm^2; the estimate obtained from the means of the samples was around 4000 to 5000 ohm cm^2. It is interesting that this last range of values for the membrane resistivity, taken together with the membrane time constant estimate of around 4 to 5 msec, implies a membrane capacity around one microfarad per cm^2; this is the same value, as noted by Dr. Cole,[5] that has been found for many different cells. Nevertheless, it must be emphasized that these estimates for cat motoneurons are subject to numerous uncertainties (see Rall, 1959, for discussion). The theoretical methods used to analyse these experimental data are, of course, applicable also to other neuron types.

SYNAPTIC EXCITATION AND INHIBITION

By means of the next few illustrations, I wish to indicate a simplified treatment of the problem of synaptic excitation and inhibition. A small patch of dendritic membrane is represented by the equivalent circuit shown in Fig. 5; synaptic excitation is treated as a step increase of the conductance, G_e, with E_e assumed to be a constant close to zero, and synaptic inhibition is treated as a step increase of the conductance, G_j, with E_j assumed to be a constant close to E_r, the resting battery. This model is based upon those of Fatt and Katz (1953) and of Coombs, Eccles and Fatt (1955); it is related to the important papers of Hodgkin and Katz (1949), Fatt and

[5] See preceding paper by Dr. K. S. Cole.

Katz (1951), and Hodgkin and Huxley (1952), as well as the earlier contributions made by Dr. Cole and others. In the mathematical model used here, it should be emphasized that G_e and G_j are assumed to undergo only step changes intended to approximate distributed synaptic activity; they are not treated as functions of potential and time as in the Hodgkin and Huxley (1952) model of the nerve impulse. Thus the mathematical model remains a partial differential equation with constant coefficients; this makes it easier to treat the effect of non-uniform distributions of such synaptic excitation and inhibition over the soma-dendritic surface of a neuron.

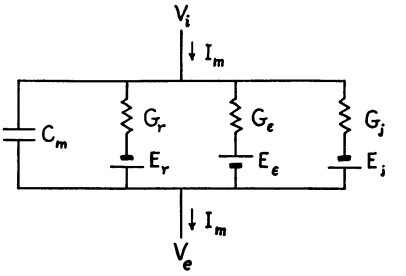

FIGURE 5 Diagram of electric model of nerve membrane; see text.

In the first example, we consider only synaptic excitation and we consider the total soma-dendritic surface as divided into two regions of equal area. The central region, which includes the soma and central portions of the several dendritic trees, is assumed to extend from $Z = 0$ to $Z = 0.5$ (a radial distance of about 500 microns in the example of Rall, 1961, Table I); see also Fig. 3-B, above; the other region is composed of the dendritic periphery and is assumed to extend from $Z = 0.5$ to $Z = 1$ (i.e., from a radial distance of about 500 microns to a radial distance of about 800 microns in the same example). It is assumed that the conductance, G_e, increases suddenly from zero to twice G_r over one of these two regions, while G_e remains zero over the other.[6] The uppermost curve in Fig. 6-A shows the transient development of depolarization to be expected at the soma if this conductance increase occurs in the central half of the receptive surface, while the lowermost curve in Fig. 6-A shows the transient response to be expected at the soma if this conductance increase occurs in the peripheral half of the receptive surface. The intermediate curve resembles the transient that would occur if the conductance, $G_e = G_r$, were uniform over the entire soma-dendritic surface.

The inset, Fig. 6-B, shows the corresponding transients for a square conductance pulse (step increase followed by a step decrease) with a duration equal to one fifth of the resting membrane time constant. Thus, Fig. 6-B provides a rough ap-

[6] Both the mathematical statement and the solution of this boundary value problem are presented elsewhere (Rall, 1961). The transient component of the solution is expressed as a convergent series of exponential terms. For the numerical examples that have been considered, this convergence was such that only the first three terms of the series needed to be considered.

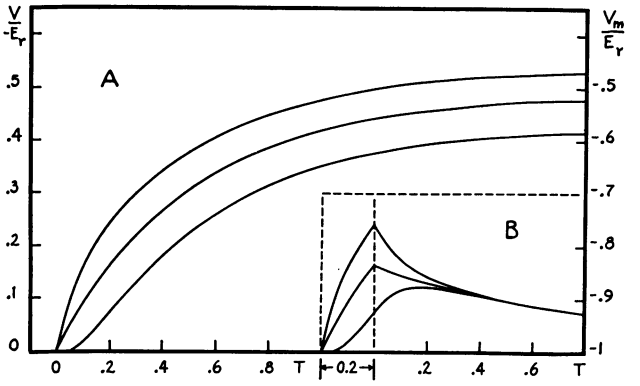

FIGURE 6 Transients of membrane depolarization in response to a sudden increase of excitatory conductance in only one half (central or peripheral) of a branching dendritic membrane surface. In (A), the conductance, G_e, increases suddenly from zero to twice G_r and remains constant at this value; in (B), this conductance first increases and then decreases suddenly back to zero after a time interval equal to 1/5 the passive membrane time constant. In both (A) and (B), the uppermost curve shows the soma membrane depolarization when the conductance change occurs in the central half of the branching system, and the lowermost curve shows the soma membrane depolarization when the conductance change occurs in the peripheral half of the branching system. The intermediate curve (in both cases) corresponds to the membrane depolarization occurring at the mid-point ($Z = 0.5$) of the branching system.

proximation to the synaptic potential produced by brief synaptic excitation, while Fig. 6-A provides an approximation to the onset of sustained synaptic activity.

These theoretical results contain several points of physiological interest. For the centrally distributed excitatory conductance increase, the initial rate of soma membrane depolarization is twice as great as when the same amount of excitatory conductance is distributed uniformly over the receptive surface. However, for the peripherally distributed conductance increase, there is a zero initial rate of soma membrane depolarization. In the case of the square conductance pulse, this particular example shows a peak soma membrane depolarization that is twice as great for the centrally distributed case as for the peripherally distributed case. This could easily represent the difference between success or failure in the initiation of an axonally propagated action potential.

In contrast to these transient phenomena, it can also be seen that the steady depolarization of the soma membrane produced by sustained G_e is only about 20 percent less for the peripherally distributed case as compared with the centrally distributed case. This suggests a need for modification of the widely held belief that synaptic excitation delivered to the dendritic periphery could produce no significant passive electrotonic spread of membrane depolarization to the soma. On the contrary, because of the very large dendritic surface area and the high density of synap-

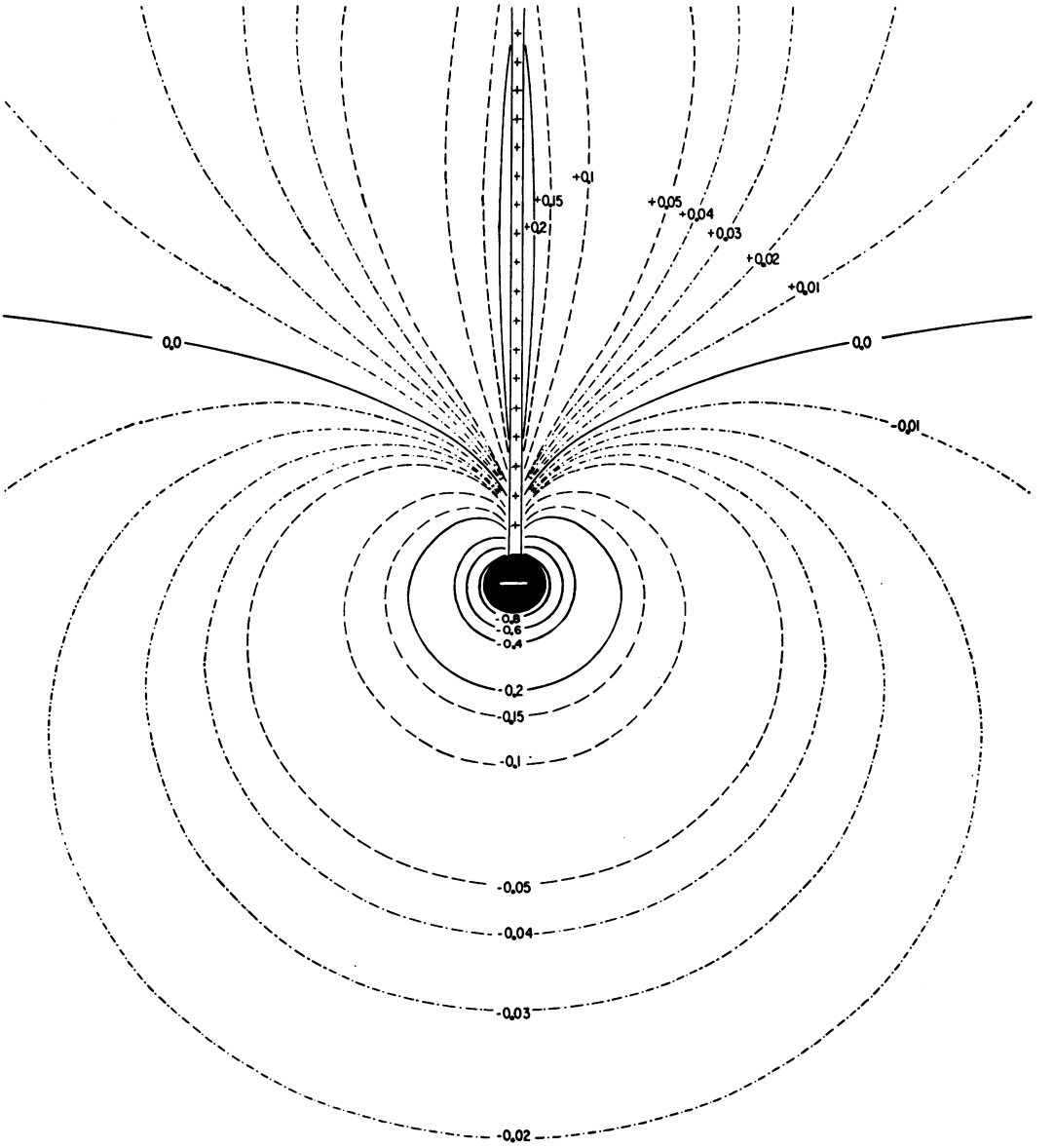

FIGURE 7 Theoretical map of isopotential contours which describe the distribution of extracellular potential corresponding to a flow of extracellular current from a single passive dendritic cylinder to a spherical soma. The distribution of dendritic source density corresponds approximately to that which can be calculated for the moment of a peak action potential in the soma. See text, and footnote 7.

tic contacts over the entire soma-dendritic surface (e.g., Wyckoff and Young, 1956; Rasmussen, 1957; Young, 1958), dendritic synaptic activity would be expected to dominate the slowly changing background level of the neuron's excitatory state. A relatively small number of (synchronously active) somatic synapses would seem to be especially well suited for precise timing (triggering) of nerve impulse initiation.

When an inhibitory conductance increase is superimposed upon an excitatory conductance increase, this is found to have a relatively small effect upon the initial rate of depolarization (Rall, 1961, Figs. 3, 8 and 9); however the amount of sustained depolarization is significantly decreased. This suggests that synaptic inhibition may operate mainly by decreasing the background level of the neuron's excitatory state; however, it is possible that synchronous, centrally located, inhibitory synaptic activity could be used to produce a precisely timed prevention of near threshold reflex discharge. The results of this section are subject to reassessment if the excitatory and inhibitory conductances of the dendritic membrane are found to exhibit significant voltage dependence; also, this model does not pretend to treat other possible mechanisms of synaptic inhibition.

DISTRIBUTION OF EXTRACELLULAR POTENTIAL

Now I wish to consider briefly the distribution of extracellular potential associated with dendritic model neurons. As a step toward this objective, Fig. 7 indicates theoretically calculated isopotential surfaces for the special case of a spherical soma and a very long cylindrical dendrite. This particular field is intended to correspond to that which occurs at the time of peak of an action potential assumed to be generated in the soma membrane; it is also assumed that the cylindrical dendritic membrane remains completely passive, and that the extracellular volume can be treated as a homogeneous, purely resistive medium. This problem is mathematically similar to certain problems of classical electrostatics, except that here the distribution of point sources along the dendritic axis is taken from the theoretical solution for passive dendritic electrotonus; also, for each dendritic source there is assumed to be a matching somatic sink.[7] The computer programming (for the IBM-650 computer

[7] In order to calculate the results shown in Figs. 7, and 9–11, it was necessary to use some particular value for the ratio of the dendritic characteristic length, λ, to the radius of the soma; in these figures, a value of 40 was used for this ratio; thus, for example, a soma radius of 35 microns would be associated with a value of 1.4 mm for λ. Also, in Figs. 7, 9 and 10, the numbers which label the isopotential contours correspond strictly to the quantity, $V_e/(I_N R_e/4\pi b)$, where I_N represents the total extracellular current flowing from dendrites to soma, R_e represents an effectively homogeneous extracellular specific resistivity, and b represents the soma radius. For the particular case of the peak somatic action potential in a cat motoneuron, this numerical quantity expresses the value of V_e approximately in millivolts. This is because of the following order of magnitude considerations: I_N is of the order, 10^{-7} ampere, because the peak intracellular action potential is of the order 10^{-1} volt, and the whole neuron instantaneous conductance is of the order, 10^{-6} ohm; $R_e/4\pi b$ is of the order, 10^{4} ohm, because the soma radius, b, lies between 25 and 50 microns, and the effective value of R_e probably lies between 250 and 500

at the National Institutes of Health), as well as other details in the preparation of Figs. 7 and 9 were done in collaboration with Mr. Ezra Shahn and Mrs. Jeanne Altmann.

The next figure (Fig. 8) indicates the orientation (but not the length) of seven cylindrical dendrites attached to a spherical soma. Relative to one dendrite at the north pole, there are three equally spaced at an angle of 60°, and there are three more at the equator. It is merely a computational chore to calculate the distribution of extracellular potential of such an array of seven dendrites from the distribution

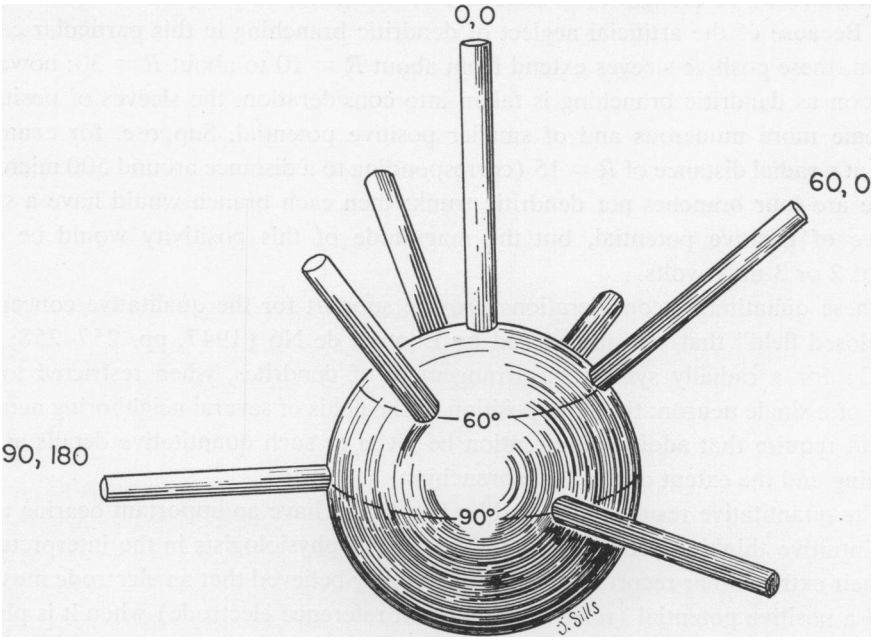

FIGURE 8 Diagram indicating the specific orientation of seven dendritic cylinders that was used in calculating Fig. 9. Relative to one dendrite at the north pole, three are equally spaced at an angle of 60°, and three are intermediately spaced around the equator.

that was calculated for the case of a single dendrite; this chore was performed by the IBM-650 computer. In order to sample the isopotential surfaces of this more complicated three dimensional distribution, we focus attention upon the plane which

ohm cm (Tasaki, Polley and Orrego, 1954; Freygang and Landau, 1955; Rank, personal communication). The mathematical details of these extracellular potential distributions have yet to be published; they involve Legendre polynomials. There is an inherent error that results from assuming extracellular isopotentiality for the passive dendritic electrotonic solutions which are, in turn, used to determine the dendritic source distribution for the extracellular potential calculation; this error is small, however, and could be further reduced by a method of successive approximations.

contains the polar axis together with one of the 60° dendrites and one of the equatorial dendrites. The isopotential contours obtained in this plane are illustrated in Fig. 9.

One striking result is that the extracellular potential is negative everywhere within a radial distance[8] of about $R = 8$. The magnitude of this negative potential falls from a value of around one millivolt near the soma surface to a value that is less than 50 microvolts for radial distances greater than about $R = 10$. The outer volume of positive potential is less than 10 microvolts everywhere except for restricted regions that may be thought of as cuffs or sleeves associated with each dendritic cylinder. Because of the artificial neglect of dendritic branching in this particular calculation, these positive sleeves extend from about $R = 10$ to about $R = 30$; however, as soon as dendritic branching is taken into consideration, the sleeves of positivity become more numerous and of smaller positive potential. Suppose, for example, that at a radial distance of $R = 15$ (corresponding to a distance around 500 microns) there are four branches per dendritic trunk; then each branch would have a small sleeve of positive potential, but the magnitude of this positivity would be only about 2 or 3 microvolts.

These quantitative considerations provide support for the qualitative concept of a "closed field" that was introduced by Lorente de Nó (1947, pp. 257–258; also 1953) for a radially symmetric arrangement of dendrites, when restricted to the case of a single neuron; the superposition of the fields of several neighboring neurons would require that additional attention be given to such quantitative details as cell spacing and the extent of dendritic branching.

The quantitative results illustrated by Fig. 9 also have an important bearing upon the intuitive thinking used by experimental neurophysiologists in the interpretation of their extracellular recordings. It is quite widely believed that an electrode must record a positive potential (relative to a distant reference electrode) when it is placed near a portion of membrane from which current flows into the extracellular volume; (see, for example, the fifth proposition of Brooks and Eccles, 1947, p. 252). However, Fig. 9 clearly shows negative extracellular potentials at the surface of the passive dendritic membrane, for radial distances up to $R = 8$.

An intuitive understanding of this result may be aided by the following comments. Although the total source current equals the total sink current, this current flows out of a widely distributed dendritic membrane surface with a small current density, while it flows into the relatively small soma membrane surface with a relatively large current density. Thus, if we consider the dendritic source system under the hypothetical condition in which the soma sink is translated to some distant location, we find that the dendritic membrane surface (at a distance, $R = 4$, from the

[8] It is convenient to let R express radial distance from the soma center, as a multiple of the soma radius. For a soma radius of 35 microns, the radial distance, $R = 8$, corresponds to 280 microns.

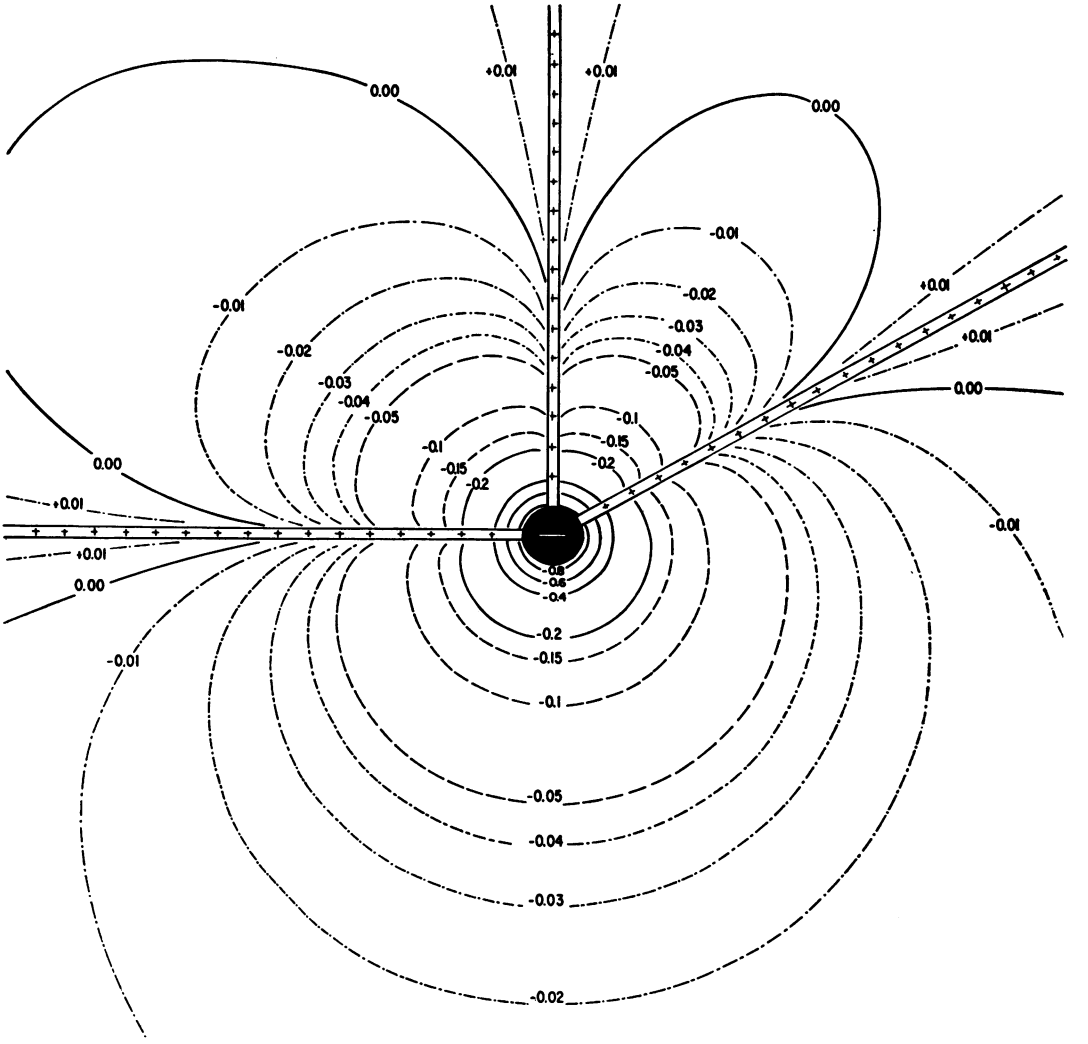

FIGURE 9 Theoretical map which samples the isopotential contours obtained for seven dendrites oriented as shown in Fig. 8; the sampling of the contours is for the plane defined by the three dendrites whose angular coordinates are indicated in Fig. 8. See discussion in text and in footnote 7; also, note that each dendrite in Fig. 9 is assumed to supply one seventh the current that is supplied by the single dendrite in Fig. 7.

center of the dendritic system) would become about 50 microvolts positive with respect to a distant reference point. However, the distant soma sink would develop a potential (relative to a distant reference point) of about −900 microvolts at its membrane surface, and about −150 microvolts at its $R = 4$. Now, when these separated source and sink systems are superimposed, the net potential (relative to a distant reference point) at the dendritic membrane surface ($R = 4$) is about −100 microvolts. Nevertheless, this portion of dendritic membrane acts as a source; the current flows out of the membrane and then flows from a potential of −100 microvolts to the soma surface potential of −800 microvolts. All this is based, however, on the assumption of an effectively homogeneous extracellular conducting medium; also, an exception should be noted explicitly for the "giant extracellular potentials."[9]

If one is willing to make the simplifying assumption of perfect radial symmetry for the extracellular potential of a stellate type dendritic neuron, one can avoid the complications of the computations involved in obtaining Figs. 7 and 9. Instead, one can compute the extracellular potential as a function of radial distance and of time, by means of the simple expression

$$V_e = \int_r^\infty \frac{I_e R_e}{4\pi\rho^2}\, d\rho$$

where I_e represents radial extracellular current, r represents radial distance from the center of the soma, and R_e is assumed to be an effectively uniform specific resistivity. If current were flowing to the soma from an infinitely distant source, I_e would be independent of r, and we would obtain a Coulomb potential (inverse proportionality with r); this has been noted by Tasaki, Polley and Orrego (1954, p. 470) and by Fatt (1957, p. 35); it is illustrated as curve D in Fig. 10. But in a dendritic neuron, the source of extracellular current (that flows into an active soma) is not infinitely distant, it is distributed (electrotonically) over the dendritic surface. In fact, our assumption of perfect radial symmetry requires us to set the radial dependence of I_e equal in magnitude (and of opposite sign) to the dependence of combined dendritic core current, I_i, upon radial distance from the soma (this was noted also by Tasaki, Polley and Orrego, 1954). This permits us to use the solutions for passive dendritic electrotonus (for both steady state or various transient conditions) to determine the radial dependence of I_e to be used in the above equation for V_e. Explicit solutions for V_e have been obtained for the case of linear and the case of exponential dependence of I_e upon radial distance; a few numerical illustrations are included in Fig. 10. It should be added that when the radial dependence of I_e is more compli-

[9] An exception must be made for "giant extracellular records" (amplitudes greater than ten millivolts from a single neuron); see for example Freygang and Frank (1959). Such potentials presumably result from additional resistance that is introduced between the microelectrode tip and the general extracellular volume; such additional resistance might be due to sharp dimpling of the cell membrane, or to penetration of a closely adjacent barrier (glial membrane?). Under such conditions, the recorded potential is dominated by the I times R drop of membrane current across this additional resistance.

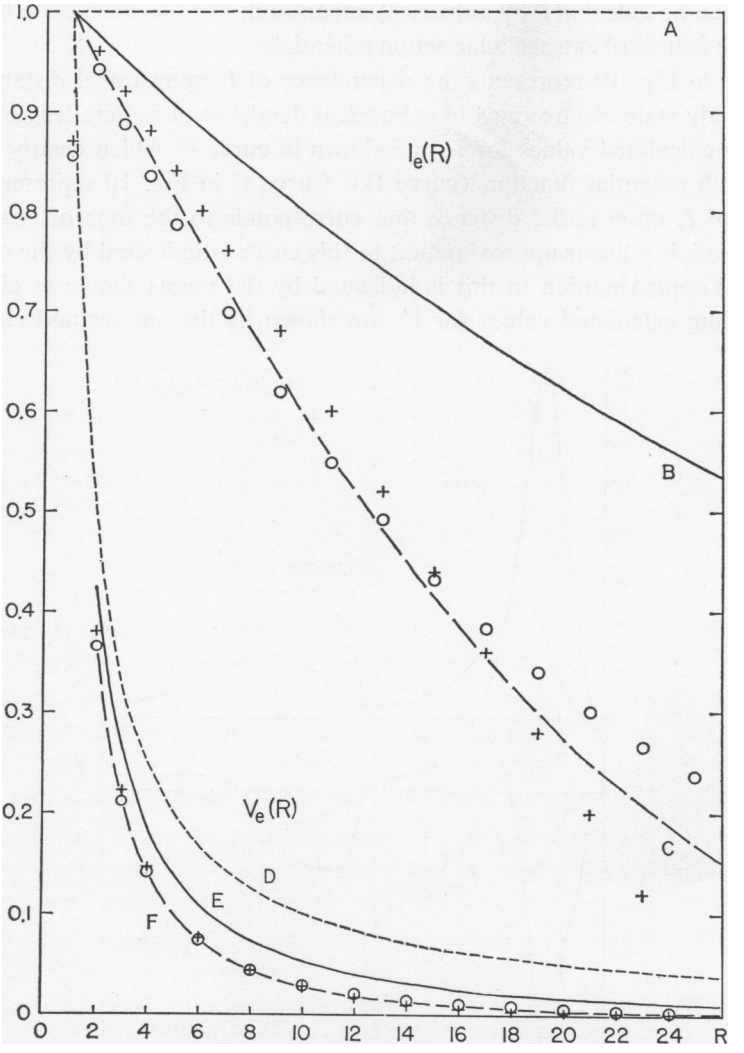

FIGURE 10 Relation between extracellular potential, V_e, and extracellular current, I_e, on the assumption of perfect radial symmetry. Curves (A) and (D) correspond to current flowing from a source at infinite distance to a spherical soma whose radius corresponds to $R = 1$. Curves (B) and (E) correspond to a radial distribution of dendritic current corresponding to a steady state of passive dendritic membrane electrotonus in a cylinder of infinite length, for a characteristic length that is about forty times the soma radius. Curves (C) and (F) correspond to the distribution of dendritic current at the moment of peak action potential at the soma: (i.e., the same moment that is portrayed in Figs. 7 and 9). The circles and crosses associated with curve (C) represent a linear and an exponential approximation to this curve; the corresponding points associated with curve (F) represent the values of V_e calculated from these approximations, while curve (F) itself is taken from calculations like that leading to Fig. 9.

cated, V_e can be calculated by numerical integration; this has been done in calculating the time course of extracellular action potentials.

Curve B in Fig. 10 represents the dependence of I_e upon radial distance for the case of steady state electrotonus in cylindrical dendrites of infinite length. The corresponding calculated values for V_e are shown in curve E, which clearly lies below the Coulomb potential function (curve D). Curve C in Fig. 10 represents the dependence of I_e upon radial distance that corresponds to the time of peak somatic action potential; a linear approximation to this curve is indicated by the crosses; an exponential approximation to this is indicated by the points shown as circles. The corresponding calculated values for V_e are shown by the crosses and circles asso-

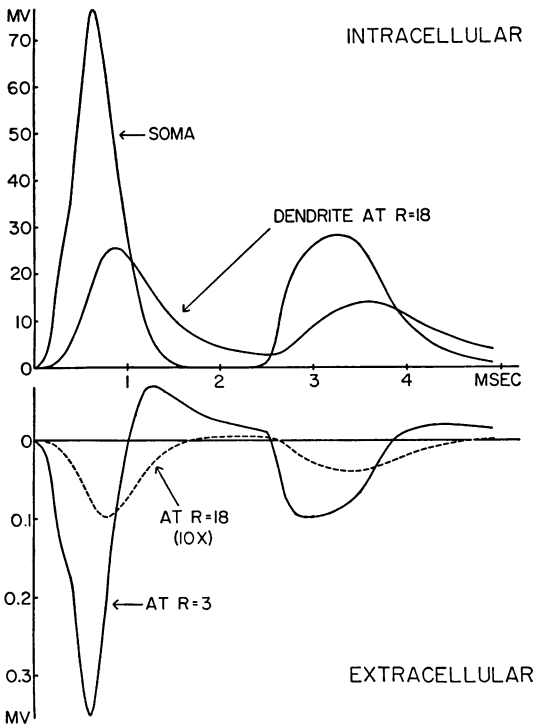

FIGURE 11 Theoretically calculated relation between intracellularly and extracellularly recorded action potentials. The uppermost curve represents an experimental "AB-spike" followed by an "A-spike" as recorded intracellularly from a cat motoneuron by Frank and Nelson. The other intracellular curve represents the theoretically calculated passive electrotonic spread into a dendritic cylinder of infinite length; it corresponds to a radial distance, R = 18 (i.e., an electrotonic distance, x/λ, of (R − 1)/40 = 0.425; this would correspond to about 600 microns in the examples mentioned elsewhere in this paper). The extracellular curves were calculated as indicated in the text and in footnote 10. The curve for R = 18 has been multiplied by ten to aid the comparison of shape. The curve at R = 3 has a shape extremely similar to that at R = 1, except that the peak at R = 1 has an amplitude about five times that at R = 3.

ciated with curve F; the broken line (curve F) has been taken from a detailed calculation of the type used to obtain Fig. 9. It may be concluded that $V_e(r)$ is not very sensitive to the difference between the linear and exponential approximations to curve C. It is also clear that curve F differs significantly from curves D and E.

Figures 7, 9 and 10 have all been concerned with the distribution of extracellular potential at one particular moment. For the case of perfect radial symmetry, it is not difficult to calculate the time course of extracellular potential at different radial distances, on the assumption that the dendrites remain completely passive while the soma membrane is treated as a voltage generator which produces a transient identical with an intracellularly recorded experimental action potential. Some results of one such calculation[10] are illustrated in Fig. 11. Such results show that the shape of the action potential, the decrement of its amplitude with radial distance, and the increase of its spike latency with radial distance are all predicted in good approximate agreement with experiment.[11] Such agreement indicates that it is not necessary to assume active propagation of an impulse into the dendritic trees to account for such experimental observations. However, it should be added that the possibility of active propagation into the dendritic trees has not been ruled out.

FURTHER PROBLEMS

The fact that this mathematical model of dendritic neurons can account for the relation between intracellularly and extracellularly recorded action potentials and that it can also make useful predictions about non-uniform distributions of synaptic excitation and inhibition would seem to provide a basis for hoping that it can be applied to additional problems of neurophysiological interest. For example, the difference found between the sluggish response to peripheral dendritic synaptic activity as compared with the much more rapid response to somatic (and dendritic trunk) synaptic activity permit a generalization of earlier reflex input-output models (e.g., Rall, 1955). This distinction between dendritic and somatic synaptic activity may prove to be particularly important for formulations of neuronal interactions

[10] The intracellular action potential (provided by Frank and Nelson) was approximated by a set of fifty voltage steps at intervals of 0.1 msec. Using the theoretical expression for electrotonic spread into a passive membrane cylinder for a voltage step applied at one end, the dependence of the membrane potential and the dendritic core current upon X and T were numerically calculated for the set of fifty voltage steps. Then, the assumption of extracellular radial symmetry permitted the extracellular potential (as a function of R and T) to be calculated by means of a numerical integration. The numerical calculations were carried out with an IBM-650 computer; I wish to express my thanks to the NIH computer programming staff for their cooperation.

[11] These comparisons between theoretical predictions and experimental results with single cat motoneurons are being carried out in cooperation with Drs. Frank and Nelson. Some additional details will be included in brief papers contributed to this Congress; full details are to be published later. The earlier work of Fatt (1957) is particularly relevant to this study. Recent experimental observations of Terzuolo, and also of Tasaki (both personal communications) appear to provide evidence for impulse propagation into a dendritic trunk.

in large populations; in the "neuronic equations" of Caianiello (1961), this would show up in the coefficients that correspond to delayed coupling.[12]

Neuroanatomists have been giving increasing attention to the large amount of overlap that exists between the fields of dendritic distribution of neighboring cells (Braitenberg and Lauria, 1961; cf. also Sholl, 1953, 1955a). One question that is usually asked is whether it is physically realistic to think in terms of a coupling between such neurons by means of the effects of extracellular potential gradients. A theoretical approach to this question can begin with the problem of expressing any given extracellular potential gradient as a gradient with respect to the electrotonic distance, Z, of the dendritic tree in question. This can then be imposed as a boundary condition for a solution of the distribution of dendritic core current and membrane potential. If we consider, for example, a dendritic neuron similar to that in the numerical example of (Rall, 1961, Table I), a preliminary calculation indicates that a constant extracellular gradient of 5 mV/mm could modify the soma membrane potential by as much as 1 mV for a favorable (asymmetric) orientation of the several dendritic trees. Relative to a threshold amount of soma membrane depolarization (around 25 mV), the above effect would be expected to produce a change in the firing probability of this neuron (see Rall and Hunt, 1956, Figs. 6, 7 and 8), or to modify the frequency of firing during a period of sustained activity (see Terzuolo and Bullock, 1956). It must be pointed out, however, that the numerical results cited above would be different for cells of different size; also, the magnitude of extracellular potential gradient that can be produced in a local region by simultaneous activity in many neighboring cells requires careful calculation.

At the beginning of this talk, I remarked that the dendritic neuron model may have relevance even to the problem of learning. What I had in mind was the growth of dendritic trees and the possibility that learning might involve preferential enlargement of certain dendritic branches.[13] It seems reasonable to suppose that different dendritic trees (or portions of these trees) provide the receptive surface for synaptic activity of different functional pathways to which a given neuron may belong. Conditioning and learning might involve an increase in the caliber and surface area of

---

[12] These are the coefficients which, in Caianiello's notation, correspond to h different from k, together with r greater than zero.

[13] The fact that dendritic trees grow during the growth and development of the organism is well known to anatomists. An example of quantitative evidence for this is provided by the factor of two found in a comparison of several human infant motoneurons with several human adult motoneurons (Rall, 1959, Table 2). Subsequent to the preparation of this manuscript, Dr. P. G. Nelson brought the recent observations of Rose *et al.* (1960) to my attention. These authors have observed significant dendritic growth during the recovery of rabbit cortex (adult as well as infant) from localized lesions; they feel that their results suggest that this "growth is actually due to a *normal, continuous growth of central neurons*". These authors also review earlier literature on the subject of neuronal growth. Also, see Sperry (1958) and Eccles (1953) for discussion (and additional references) on the subject of physiological plasticity and neuronal connectivity.

the appropriate dendritic branches. This would enhance the synaptic effectiveness of this pathway in at least two ways: it would provide additional surface for either additional or larger synaptic terminals; at the same time, the enlarged caliber of these branches (and perhaps of their trunk) would increase the amount and rate of electrotonic spread from this region to the central convergence zone (at or near the soma). Thus, the influence of this entire synaptic and dendritic system would be increased. Although, it seems very likely that there is some effect of this kind, at least during growth, the critical question would seem to concern the magnitude and reliability of such changes; the most severe question, of course, is whether such changes actually do underlie learning. With regard to this last question, my suggestion is purely speculative; however, I think it merits consideration with other specific suggestions, such as the earlier suggestion that a swelling of synaptic knobs might underlie the plasticity of the nervous system (Eccles and Rall, 1951, pp. 373–375; see also Eccles, 1953; pp. 198 and 216–226). It may be noted that dendritic branch growth would share with synaptic knob growth the important property of being located upstream from the central convergence zone of the neuron. This property insures an important specificity to the active pathway; this specificity would be lost if the change took place at the convergence zone (i.e., at the soma). However, in the case of dendritic growth, this specificity would not be absolute; another pathway which happens to involve synapses to the same dendritic branches would also benefit from the enhanced electrotonic spread to the soma. If this other pathway happened to be the one to be conditioned, this overlap could add significantly to the efficiency of the conditioning process.

It is interesting that the concept of the soma (perikaryon) as the convergence zone for effects produced in the dendrites dates back more than fifty years to the work of Sherrington and Ramón y Cajal (see pp. 143–144 of the 1947–48 edition of Sherrington, 1906). At that time, however, nervous activity was not yet viewed in terms of nerve membrane disturbances.

SUMMARY

The development of a mathematical model of dendritic neurons is reviewed briefly. This model is used as the basis for quantitative interpretations of recent electrophysiological measurements made on single dendritic neurons by means of intracellular and extracellular microelectrodes; specific examples are given for motoneurons of cat spinal cord. A simplified treatment of synaptic excitation and inhibition leads to the theoretical prediction of a functional distinction between somatic and dendritic synapses: dendritic synaptic activity would be expected to dominate slow adjustments of the background excitation level, while somatic synapses would be best suited for triggering of impulses. Theoretical distributions of extracellular potential are presented for the case of a completely passive dendritic membrane associated with an action potential generated by the soma mem-

brane; some of the implications of these results for the intuitive approach to neurophysiological interpretations are discussed. Also, the time course and the dependence upon radial distance of such extracellular action potentials are found to be in good agreement with experiment. The relevance of this dendritic neuron model to such further problems as neuronal interactions and the plastic changes underlying learning is discussed.

REFERENCES

AITKEN, J. T., (1955). Observations on the larger anterior horn cells in the lumbar region of the cat's spinal cord. *J. Anat., Lond.* **89:** 571.

AITKEN, J. T. and BRIDGER, J. E., (1961). Neuron size and neuron population density in the lumbosacral region of the cat's spinal cord. *J. Anat., Lond.*, **95:** 38–53.

ARAKI, T., and OTANI, T., (1955). Response of single motoneurons to direct stimulation in toad's spinal cord. *J. Neurophysiol.* **18:** 472–485.

BISHOP, G. H., (1958). The dendrite: receptive pole of the neurone. *EEG Clin. Neurophysiol. Suppl. No. 10:* 12–21.

BRAITENBERG, V., and LAURIA, F., (1961). Toward a mathematical description of the grey substance of nervous systems. *Nuovo Cim.* In press.

BROOKS, C. McC., and ECCLES, J. C., (1947). Electrical investigation of the monosynaptic pathway through the spinal cord. *J. Neurophysiol.*, **10:** 251–274.

BULLOCK, T. H., (1959). Neuron doctrine and electrophysiology. *Science,* **129:** 997–1002.

CAIANIELLO, E. R., (1961). Outline of a theory of thought processes and thinking machines. *J. Theoret. Biol.*, **1:** 204–235.

COOMBS, J. S., CURTIS, D. R., and ECCLES, J. C., (1959). The electrical constants of the motoneurone membrane. *J. Physiol., Lond.* **145:** 505–528.

COOMBS, J. S., ECCLES, J. C. and FATT, P., (1955). The inhibitory suppression of reflex discharges from motoneurones. *J. Physiol.*, **130:** 296–413.

DAVIS, L. JR. and LORENTE DE NÓ, R., (1947). Contribution to the mathematical theory of the electrotonus. *Stud. Rockefeller Inst. M. Res.* **131:** 442–496.

ECCLES, J. C., (1953). "The neurophysiological basis of mind", London, Oxford.

ECCLES, J. C., and RALL, W., (1951). Effects induced in a monosynaptic reflex path by its activation. *J. Neurophysiol.*, **14:** 353–376.

FATT, P., (1957). Electrical potentials occurring around a neurone during its antidromic activation. *J. Neurophysiol.* **20:** 27–60.

FATT, P. and KATZ, B., (1951). An analysis of the end-plate potential recorded with an intracellular electrode. *J. Physiol.*, **115:** 320–370.

FATT, P. and KATZ, B., (1953). The effect of inhibitory nerve impulses on a crustacean muscle fibre. *J. Physiol.*, **121:** 374–389.

FOX, C. A. and BARNARD, J. W., (1957). A quantitative study of the Purkinje cell dendritic branchlets and their relationship to afferent fibres. *J. Anat., Lond.*, **91:** 299–313.

FRANK, K. and FUORTES, M. G. F., (1956). Stimulation of spinal motoneurones with intracellular electrodes. *J. Physiol., Lond.* **134:** 451–470.

FREYGANG, W. H., JR., and FRANK, K. (1959). Extracellular potentials from single spinal motoneurons. *J. Gen. Physiol.* **42:** 749–760.

FREYGANG, W. H., JR., and LANDAU, W. M., (1955). Some relations between resistivity and electrical activity in the cerebral cortex of the cat. *J. Cell. Comp. Physiol.*, **45:** 377–392.

HODGKIN, A. L. and HUXLEY, A. F., (1952). A quantitative description of membrane current and its application to conduction and excitation in nerve. *J. Physiol.*, **117:** 500–544.

HODGKIN, A. L. and KATZ, B., (1949). The effect of sodium ions on the electrical activity of the giant axon of the squid. *J. Physiol.*, **108:** 37–77.

HODGKIN, A. L. and RUSHTON, W. A. H., (1946). The electrical constants of a crustacean nerve fibre. *Proc. Roy. Soc. B. Lond.*, **133**: 444–479.

LORENTE DE NÓ, R., (1947). Action potential of the motoneurons of the hypoglossus nucleus. *J. Cell. Comp. Physiol.*, **29**: 207–287.

LORENTE DE NÓ, R., (1953). Conduction of impulses in the neurons of the oculomotor nucleus. In "The Spinal Cord", Ciba Found. Symposium; Editors: J. L. Malcolm and J. A. B. Gray. Little, Brown, Boston.

RALL, W., (1955). A statistical theory of monosynaptic input-output relations. *J. Cell. Comp. Physiol.*, **46**: 373–411.

RALL, W., (1959). Branching dendritic trees and motoneuron membrane resistivity. *Exp. Neurol.*, **1**: 491–527.

RALL, W., (1960). Membrane potential transients and membrane time constant of motoneurons. *Exp. Neurol.*, **2**: 503–532.

RALL, W., (1961). Theory of physiological properties of dendrites. *Ann. N. Y. Acad. Sci.*, in press, (Vol. 96).

RALL, W., and HUNT, C. C., (1956). Analysis of reflex variability in terms of partially correlated excitability fluctuations in a population of motoneurons. *J. Gen. Physiol.*, **39**: 397–422.

RAMÓN Y CAJAL, S., (1909). "Histologie du système nerveux de l'homme et des vertébrés," vol. 1, Paris, Maloine.

RASMUSSEN, G. L., (1957). In "New Research Techniques of Neuroanatomy", edited by W. F. Windle, Charles Thomas, Springfield, Illinois.

ROSE, J. E., MALIS, L. E., KRUGER, L. and BAKER, C. P., (1960). Effects of heavy, ionizing, monoenergetic particles on the cerebral cortex. II. *J. Comp. Neurol.*, **115**: 243–255.

SHERRINGTON, C. S., (1906). "The integrative action of the nervous system". Scribners, New York. Second edition (1947), Yale Univ. Press.

SHOLL, D. A., (1953). Dendritic organization in the neurons of the visual and motor cortices of the cat. *J. Anat., Lond.*, **87**: 387–406.

SHOLL, D. A., (1955a). The organization of the visual cortex in the cat. *J. Anat., Lond.* **89**: 33–46.

SHOLL, D. A., (1955b). The surface area of cortical neurons. *J. Anat., Lond.*, **89**: 571–572.

SPERRY, R. W., (1958). Physiological plasticity and brain circuit theory. In "Biological and biochemical bases of behavior." Ed. H. F. Harlow and C. N. Woolsey. Univ. Wisconsin Press, Madison.

TASAKI, I., POLLEY, E. H., and ORREGO, F., (1954). Action potentials from individual elements in cat geniculate and striate cortex. *J. Neurophysiol.*, **17**: 454–474.

TERZUOLO, C. A., and BULLOCK, T. H., (1956). Measurement of imposed voltage gradient adequate to modulate neuronal firing. *Proc. Nat. Acad. Sci.*, **42**: 687–694.

WYCKOFF, R. W. G. and YOUNG, J. Z., (1956). The motorneuron surface. *Proc. Roy. Soc. B. Lond.*, **144**: 440–450.

YOUNG, J. Z., (1958). Anatomical considerations. *EEG Clin. Neurophysiol., Suppl. No. 10:* 9–11.